Anomalous chaotic atomic transport in optical lattices

Sergey Prants

Pacific Oceanological Institute, Vladivostok, Russia

Contents

- Coherent nonlinear dynamics of the atom-field interaction
- Regimes of motion
- Stochastic map for chaotic atomic transport
- Statistical properties of chaotic transport
- Quantum-classical correspondence

1 Coherent nonlinear dynamics of the atom-field interaction

A two-level atom moving in a 1D standing laser wave

$$\hat{H} = \frac{P^2}{2m_a} + \frac{1}{2}\hbar(\omega_a - \omega_f)\hat{\sigma}_z - \hbar\Omega\left(\hat{\sigma}_- + \hat{\sigma}_+\right)\cos k_f X. \tag{1}$$

Coherent evolution in the absence of any losses is governed by the Hamilton-Schrödinger equations

$$\begin{aligned} \dot{x} &= \omega_r p, \quad \dot{p} = -u\sin x, \quad \dot{u} = \Delta v, \\ \dot{v} &= -\Delta u + 2z\cos x, \quad \dot{z} = -2v\cos x, \end{aligned} \tag{2}$$

$x \equiv k_f X$ and $p \equiv P/\hbar k_f$ are classical atomic center-of-mass position and momentum, u and v are a synchronized and a quadrature components of the atomic electric dipole moment, z is the atomic population inversion. The dimensionless time $\tau \equiv \Omega t$. The normalized recoil frequency, $\omega_r \equiv \hbar k_f^2/m_a\Omega \ll 1$, and the atom-field detuning, $\Delta \equiv (\omega_f - \omega_a)/\Omega$, are the control parameters.

Two integrals of motion: $H \equiv \frac{\omega_r}{2}p^2 - u\cos x - \frac{\Delta}{2}z$ and the Bloch vector $u^2 + v^2 + z^2 = 1$.

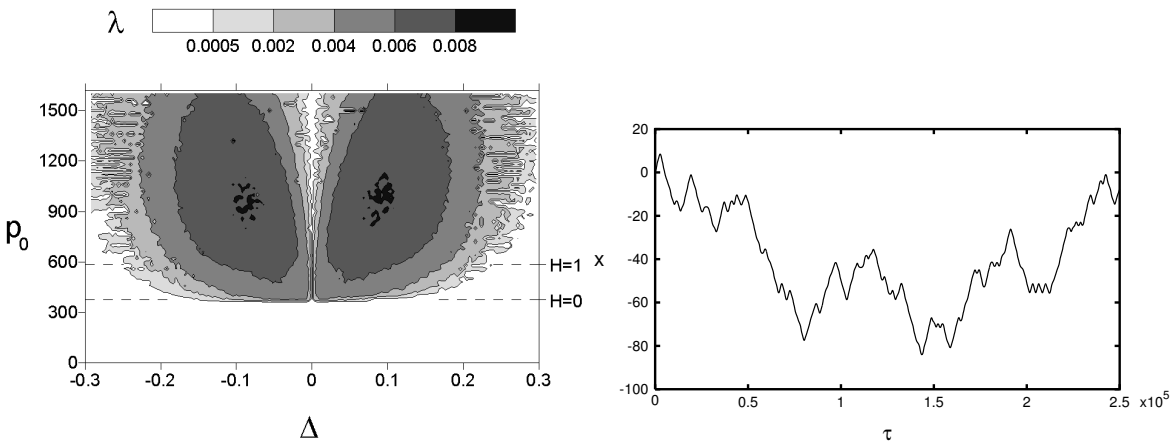

Figure 1: **Left: maximum Lyapunov exponent λ vs atom-field detuning Δ and initial atomic momentum p_0. Right: typical atomic trajectory in the regime of chaotic transport, $\omega_r = 10^{-5}$.**

2 Regimes of motion

At zero detuning, the fast (u, v, z) and slow (x, p) variables are separated allowing one to integrate exactly the equations of motion. Off the resonance, atoms may wander in a chaotic way in the optical lattice with alternating trappings in the wells of the optical potential and flights over its hills (Argonov and SP, JETP 2003). The c.m. motion is described by the equation of a nonlinear physical pendulum with the frequency modulation

$$\ddot{x} + \omega_r u(\tau) \sin x = 0. \tag{3}$$

Atom moves in an optical potential $-u \cos x$, a nonstationary structure with potential wells of different depths.

3 Stochastic map for chaotic atomic transport

Chaotic atomic transport may occur even if the detuning is very small, $|\Delta| \ll 1$ (Fig. 1). At $|\Delta| \neq 0$ and far from the nodes, the variable u performs shallow oscillations. "Jumps" of u are expected to occur near the nodes. Approximating the variable u between the nodes by constant values, we construct a discrete stochastic mapping (Argonov and SP, PRA 2007)

$$u_m = \sin(\Theta \sin \varphi_m + \arcsin u_{m-1}), \tag{4}$$

where $\Theta \equiv |\Delta|\sqrt{\pi/\omega_r p_{\mathrm{node}}}$ is an angular amplitude of the jump, u_m value of u just after the m-th node crossing, φ_m random phases, and $p_{\mathrm{node}} \equiv \sqrt{2H/\omega_r}$ the value of p when atom crosses a node (it is practically a constant with a given value of H for all the nodes).

With given values of Δ, ω_r, and $p_{\rm node}$, the map (4) has been shown numerically to give a satisfactory probabilistic distribution of magnitudes of changes in the variable u just after crossing the nodes. The stochastic map (4) is valid under the assumptions of small detunings ($|\Delta| \ll 1$) and comparatively slow atoms ($|\omega_r p| \ll 1$). It allows to reduce the basic set of equations of motion (2) to the effective equation of motion (3).

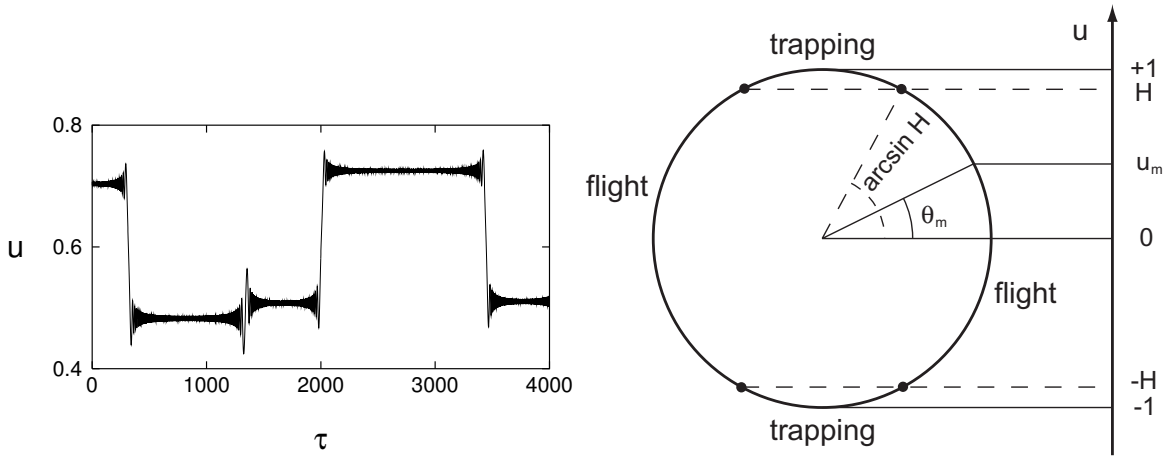

Figure 2: **Left: typical evolution of the atomic dipole-moment component u for comparatively slow and slightly detuned atom,$\Delta = -0.01$. Right: graphic representation for u_m and $\theta_m \equiv \arcsin u_m$ maps. H is a given value of the atomic energy. Atoms either oscillate in potential wells (trapping) or fly through the optical lattice (flight).**

4 Statistical properties of chaotic transport

4.1 Model for chaotic atomic transport

At $H < 0$, atom is trapped in the first well, at $H > |u|_{\max} = 1$, atom moves in the same direction, whereas at $0 < H < 1$, atom can change its direction of motion. There is a direct correspondence between chaotic atomic transport in the optical lattice and stochastic dynamics of the Bloch variable u.

Let us introduce the map for $\arcsin u_m$

$$\theta_m \equiv \arcsin u_m = \Theta \sin \varphi_m + \arcsin u_{m-1}, \tag{5}$$

which describes a random motion of the point along a circle of the unit radius (Fig. 2). The vertical projection of this point is u_m. The value of the energy H specifies four regions, two of which correspond to atomic oscillations in a well, and two other ones — to ballistic motion in the optical lattice. "A flight" is an event when atom passes, at least, two successive antinodes (and three nodes). The discrete flight length is a number of nodes l the atom crossed. Center-of-mass oscillations in a well of the optical potential will be called "a trapping".

4.2 Statistics of chaotic atomic transport at large jump magnitudes of u

If the angular amplitudes of the jumps are sufficiently large $\Theta \gtrsim \frac{\pi}{2}$, then the internal atomic variable $\theta_m \equiv \arcsin u_m$ just after crossing the m-th node may take with the same probability practically any value from the range $[-\pi/2, \pi/2]$ (see Fig. 2). With given values of the recoil frequency $\omega_r = 10^{-5}$ and the energy in the range $0 < H < 1$, large jumps take place at medium detunings $|\Delta| \sim 0.1$. The probability for an atom to cross l successive nodes before turning is

$$P_{\rm fl}(l) = {P_+}^l P_- = \left(\frac{\arccos H}{\pi}\right) \exp\left[l \ \ln\left(1 - \frac{\arccos H}{\pi}\right)\right]. \qquad (6)$$

It is a flight probability density function (PDF) in terms of the discrete flight lengths. The exponential decay means that the atomic transport is normal for sufficiently large values of the jump magnitudes of the variable u. The probability for a trapped atom to cross the corresponding well node l times before escaping from the well is

$$P_{\rm tr}(l) = {P_-}^l P_+ = \left(1 - \frac{\arccos H}{\pi}\right) \exp\left[l \ \ln\left(\frac{\arccos H}{\pi}\right)\right]. \qquad (7)$$

4.3 Statistics of chaotic atomic transport at small jump magnitudes of u

With small values of the angular amplitudes, $\Theta \ll \frac{\pi}{2}$, it may take a long time for an atom to exit from one of the trapping or flight regions in Fig. 2. The result will depend on how long is the length of the corresponding circular arc in Fig. 2 as compared with the jump lengths.

- **Jump lengths are small as compared with the lengths of both the flight and trapping arcs**

$$\Theta \ll \min\{\arcsin H, \arccos H\}. \tag{8}$$

Motion of θ_m along the circle can be treated as a one-dimensional diffusion process for a fictitious particle with the diffusion coefficient $D = \Theta^2/4$. The probability density for a particle to exit from the interval of the length $2\theta_{\max}$ after crossing l nodes is

$$P(l) \simeq \frac{Q}{\theta_{\max}^3} \sum_{j=0}^{\infty} \left(j + \frac{1}{2}\right)^2 \exp \frac{-\left(j + \frac{1}{2}\right)^2 \pi^2 D l}{\theta_{\max}^2}, \tag{9}$$

where Q is a normalization constant and $\theta_{\max}$ is equal to $\arcsin H$ for flights and $\arccos H$ for trappings.

If $l \gtrsim \theta_{\max}^2/D$, then all the terms in the sum (9) are small as compared with the first one. Both the flight and trapping statistics are exponential in this case. To the contrary, if $l \ll \theta_{\max}^2/D$, then one should take into account a large number of terms in the sum (9) and we get the power law decay

$$P(l) \simeq \frac{Q\pi^{-2.5}D^{-1.5}}{4} l^{-1.5}, \quad l \ll \frac{\theta_{\max}^2}{D} \tag{10}$$

both for the flight and trapping PDFs. The power-law statistics (10) implies anomalous atomic transport.

The size of the trapping and flight regions depends on the value of the atomic energy H (see Fig. 2). At $H > \sqrt{2}/2$ ($\arcsin H > \pi/4$), the flight PDF P_{fl} has a longer decay than the trapping PDF P_{tr}. On the contrary, at $H < \sqrt{2}/2$, the P_{tr}'s decay is longer than the P_{fl}'s one.

- **If the jump magnitude is of the order of the size of the flight or trapping regions**

$$\Theta \sim \arcsin H \ll \frac{\pi}{2} \quad \text{or} \quad \Theta \sim \arccos H \ll \frac{\pi}{2}, \tag{11}$$

then a particle may pass through the region making a small number of jumps l. So, the approximation of the diffusion process (8) fails, and the corresponding PDF is exponential.

In order to check the analytical results obtained, we compare them with numerical simulation of the reduced (3) and basic (2) equations of motion. In Fig. 3 (left) we compare the results (in a log-log scale) in the case of small jump magnitudes of the variable u ($\Delta = -0.001$) and approximately equal sizes of the flight and trapping regions ($H = 0.724 \sim \sqrt{2}/2$). The initial segment of the function demonstrate the power law decay with the slope -1.5 given by the formula (10). The central segment cannot be fitted by a simple function. In the range $l \gtrsim l_{\rm cr}^2 \simeq 3000$, the decay is expected to be purely exponential in accordance with the first term in Eq. (9).

In order to demonstrate what happens with larger values of the jump magnitudes, we take the detuning to be $\Delta = -0.01$ increasing the jump magnitude in ten times as compared with the preceding cases. With the taken value of the energy $H = 0.8055$ we provide a slight domination of flights over trappings. The jump magnitude is now so large that particles may pass through the flight and trapping regions making a small number of jumps. It is expected that all the PDFs, both the flight and trapping ones, should be practically exponential in the whole range of the crossing number l. It is really the case (see Fig. 3 (right)).

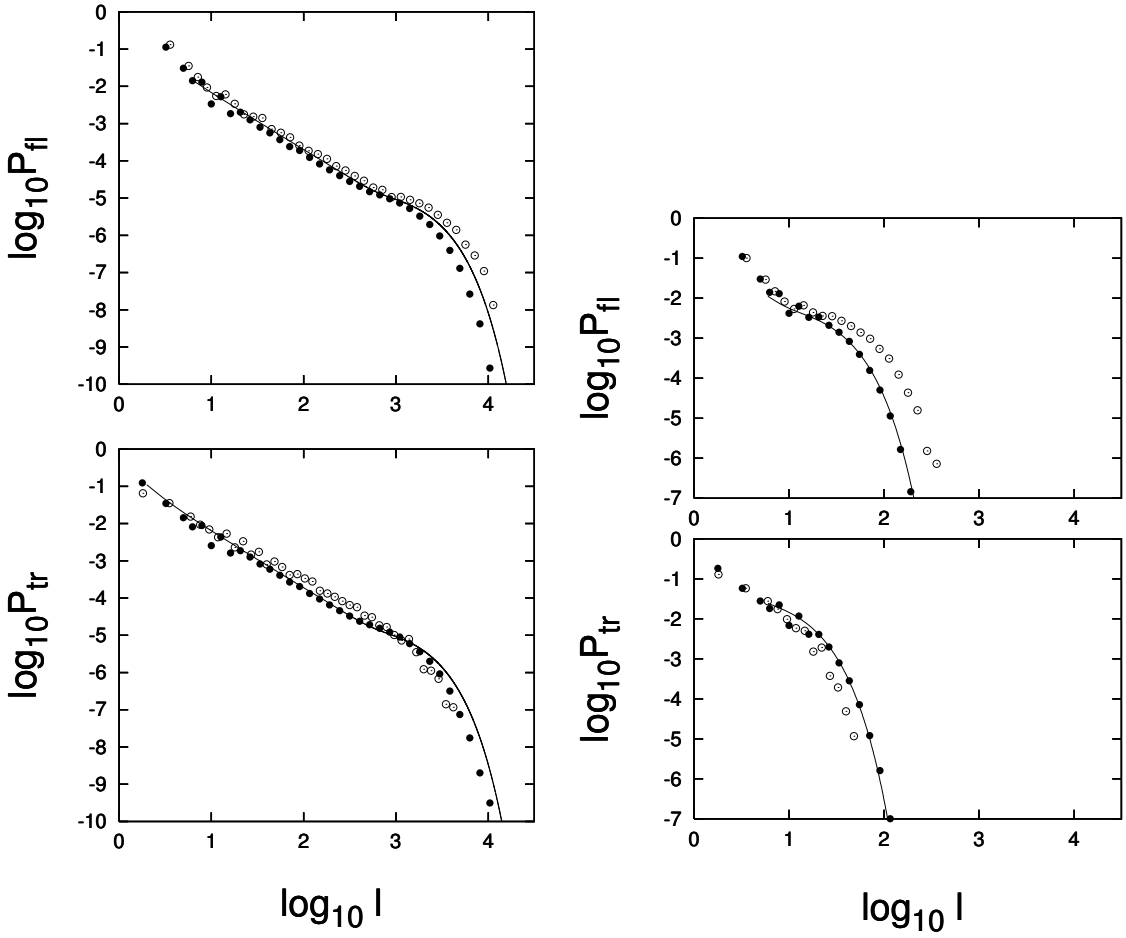

Figure 3: **Left: The flight $P_{\rm fl}$ and trapping $P_{\rm tr}$ PDFs for a chaotically moving atom with small jumps of u at $\Delta = -0.001$. The energy value $H = 0.724$ ($p_0 = 535$) provides approximately equal sizes of the flight and trapping regions in Fig. 2. Right: The same with large u-jumps at $\Delta = -0.01$. $H = 0.8055$ ($p_0 = 550$) provides a domination of the flight events over the trapping ones. White and black circles represent results of integration of the basic (2) and reduced (3) equations of motion, respectively, and the solid lines represent the analytical PDFs (9).**

5 Poincaré sections

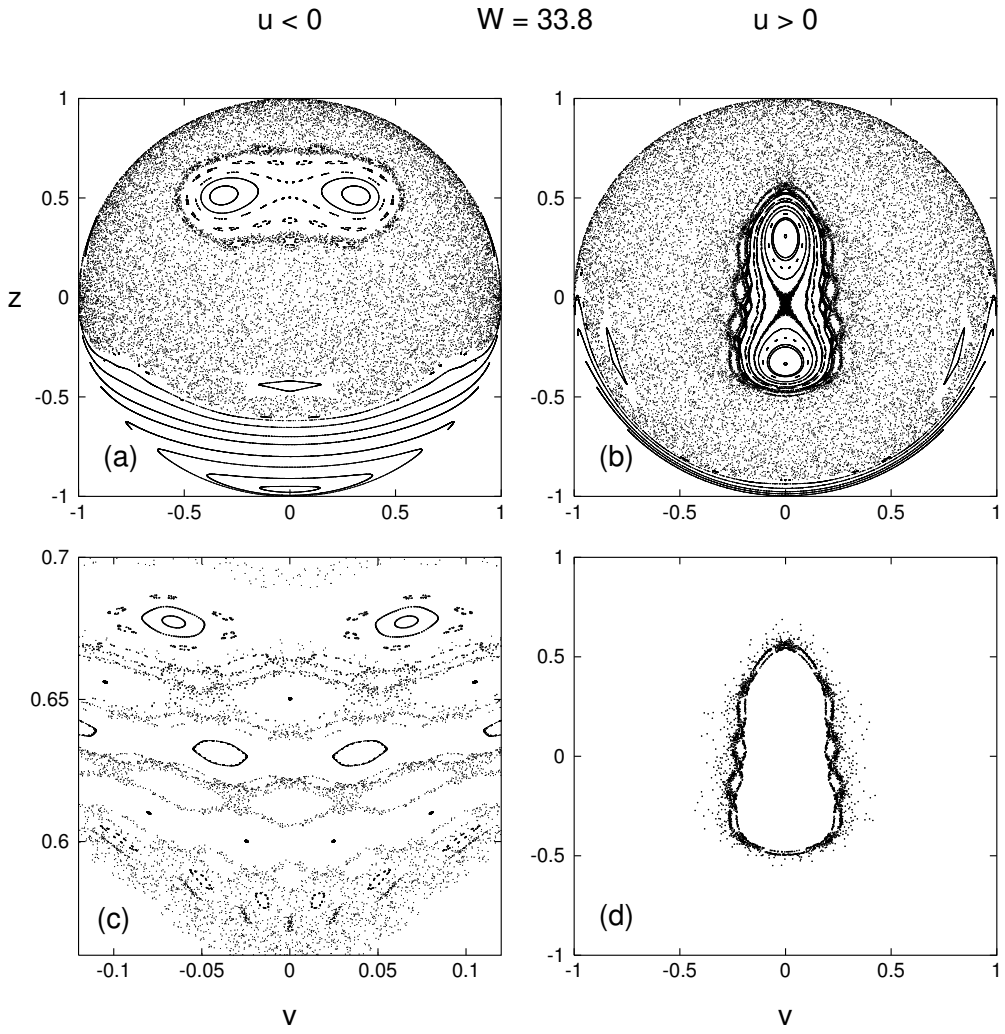

Figure 4: **Poincaré mapping in the Bloch variable space. (a)** $u < 0$, **(b)** $u > 0$, **(c) magnification of the small region in (a) fragment, (d) mapping with a single chaotic trajectory in (b) fragment, illustrating the effect of sticking:** $W = 33.8$, $p_{\text{eff}} = 2600$, $\omega_r = 10^{-5}$, $\Delta = -0.05$.

Poincaré mappings for a number of ballistic atomic trajectories in the western $(u < 0)$ **and eastern** $(u > 0)$ **Bloch hemispheres** (u, v, z) **on the plane** $v - z$. $\Delta = -0.05$, $\omega_r = 10^{-5}$, **the total energy** $W = 33.8$, $x_0 = 0$.

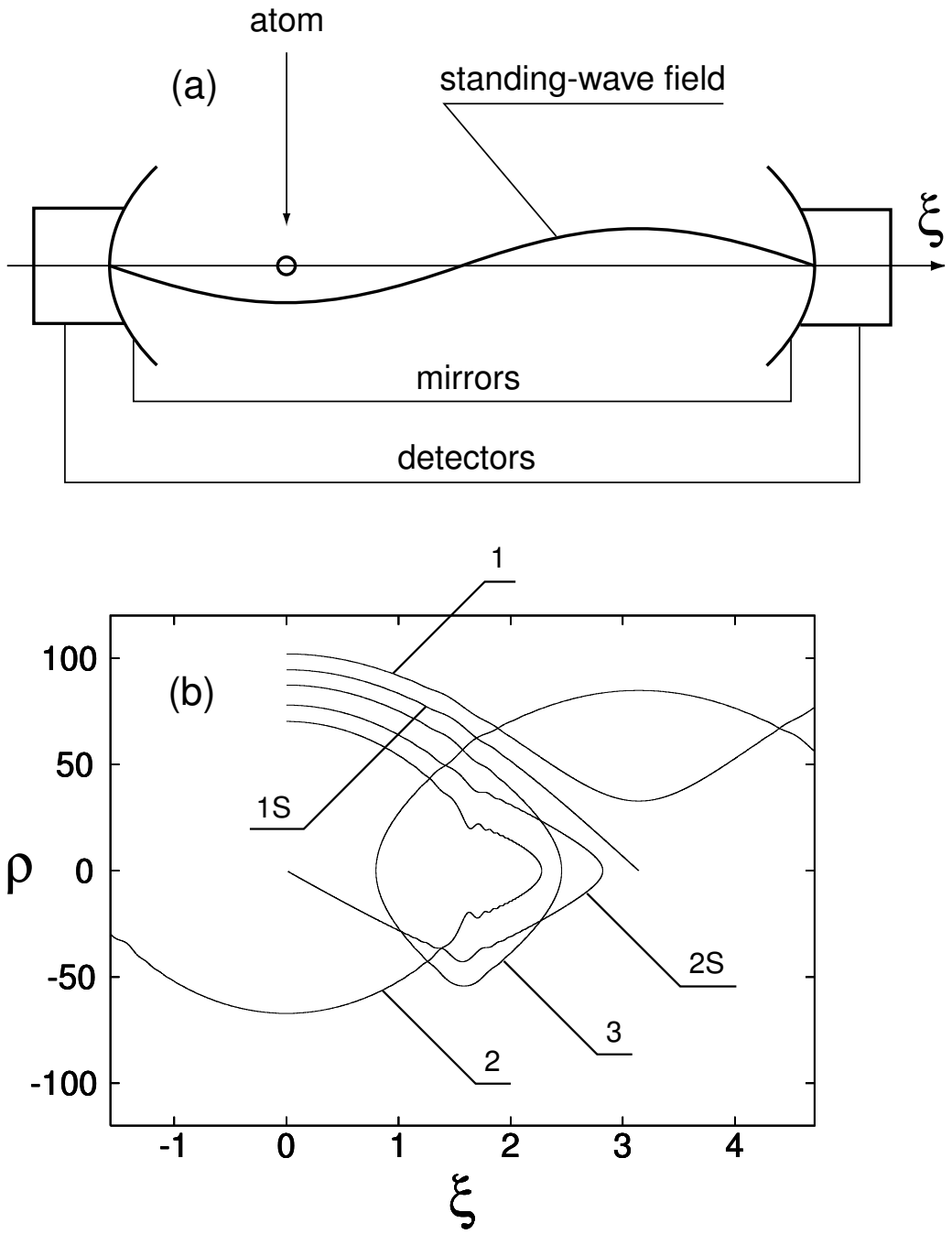

Figure 5: **The schematic diagram shows the optical lattice with detectors.**

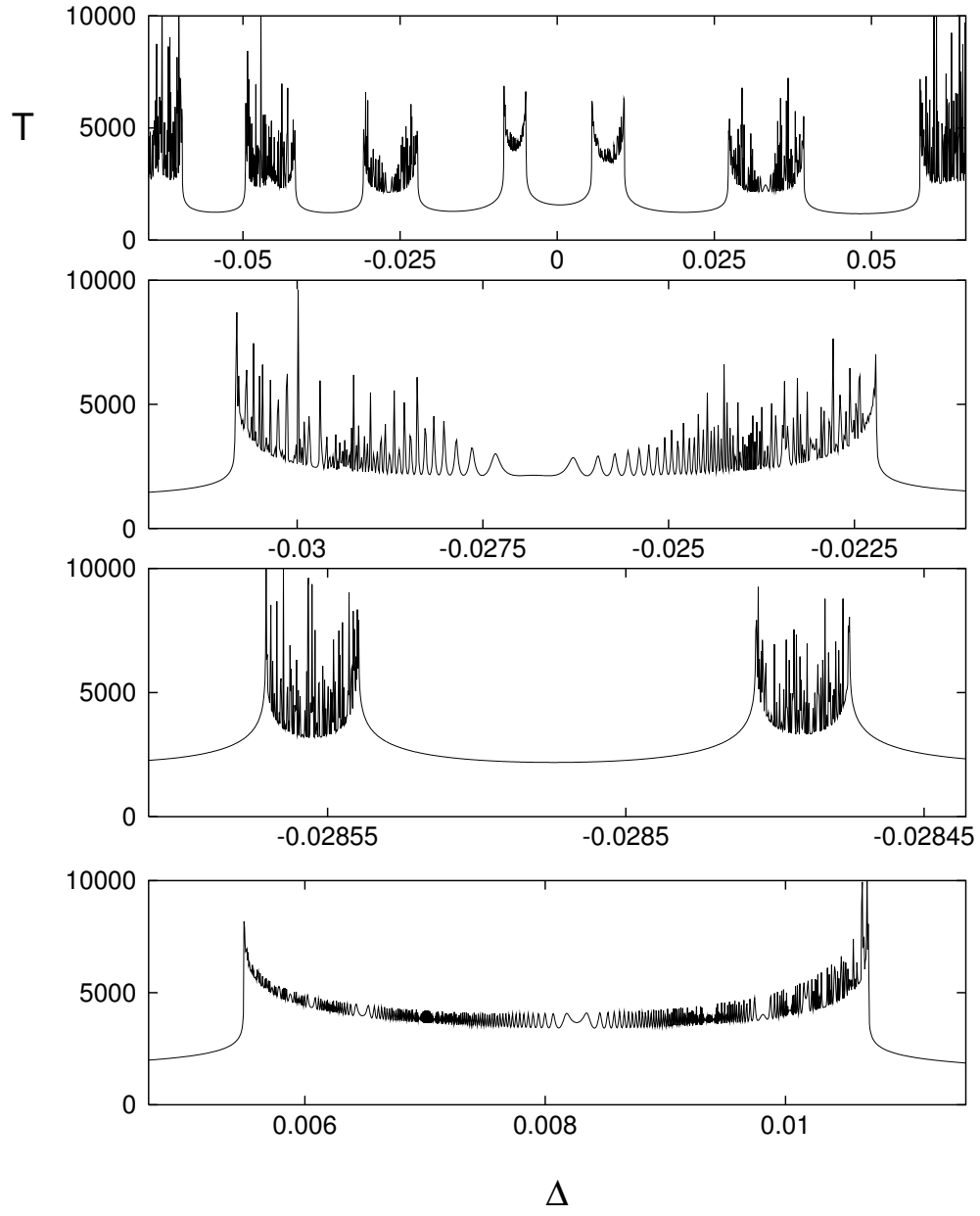

Figure 6: **Fractal-like dependence of the time of exit of atoms T (in units of Ω^{-1}) from a small region in the optical lattice on the detuning Δ (in units of Ω): $p_0 = 200$, $z_0 = -1$, $u_0 = v_0 = 0$. Magnifications of the detuning intervals are shown.**

7 Wave packet motion and quantum-classical correspondence

The Hamiltonian

$$\hat{H} = \frac{\hat{P}^2}{2m_a} + \frac{\hbar}{2}(\omega_a - \omega_f)\hat{\sigma}_z - \hbar\Omega\,(\hat{\sigma}_- + \hat{\sigma}_+)\cos k_f\hat{X}, \tag{12}$$

the state vector in the momentum representation

$$|\Psi(t)\rangle = \int [a(P,t)|2\rangle + b(P,t)|1\rangle]|P\rangle dP, \tag{13}$$

where $a(P,t)$ and $b(P,t)$ are the probability amplitudes to find atom at time t with the momentum P in the excited, $|2\rangle$, and ground, $|1\rangle$, states, respectively. The normalized Schrödinger equation for the probability amplitudes (SP, JETP 2009)

$$\begin{aligned} i\dot{a}(p) &= \frac{1}{2}(\omega_r p^2 - \Delta)a(p) - \frac{1}{2}[b(p+1) + b(p-1)], \\ i\dot{b}(p) &= \frac{1}{2}(\omega_r p^2 + \Delta)b(p) - \frac{1}{2}[a(p+1) + a(p-1)]. \end{aligned} \tag{14}$$

The probability to find an atom with the momentum p at the moment of time τ is $\mathcal{P}(p,\tau) = |a(p,\tau)|^2 + |b(p,\tau)|^2$. The internal atomic state is described by the following real-valued combinations of the probability amplitudes: $u(\tau) \equiv 2\,\mathrm{Re}\int dp\,[a(p,\tau)b^*(p,\tau)]$, $v(\tau) \equiv -2\,\mathrm{Im}\int dp[a(p,\tau)b^*(p,\tau)]$, $z(\tau) \equiv \int dp[|a(p,\tau)|^2 - |b(p,\tau)|^2]$, which are expected values of the synchronized (with the laser field) and a quadrature components of the atomic electric dipole moment (u and v, respectively) and the atomic population inversion, z.

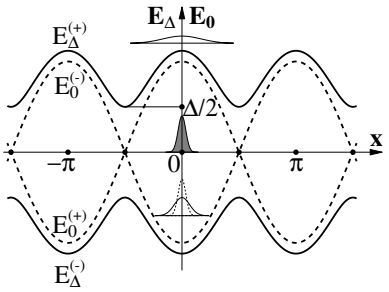

Probability to make a nonadiabatic transition

$$P_{LZ} = \exp(-\kappa), \tag{15}$$

from one of the nonresonant potentials to another one specified by the Landau–Zener parameter

$$\kappa \equiv \pi \frac{\Delta^2}{\omega_D}, \tag{16}$$

The quantity $\omega_r|p_{\rm node}|$ is a normalized Doppler shift for an atom moving with the momentum $|p_{\rm node}|$, i.e., $\omega_D \equiv \omega_r|p_{\rm node}| \equiv k_f|v_{\rm node}|/\Omega$.

There are three regimes of atomic motion.

- $\kappa \gg 1$. **The probability to make the transition is exponentially small even when an atom crosses a node. The evolution of the atomic wave packet is adiabatic in this case.**
- $\kappa \ll 1$. **The distance between the potentials at the nodes is small and the atom changes the potential each time when crossing any node with the probability close to unity. In the limit case $\Delta = 0$, the atom moves in the resonant potentials.**
- $\kappa \simeq 1$. **The probability to change the potential or to remain in the same one, upon crossing a node, are of the same order. In this regime one may expect a proliferation of components of the atomic wave packet at the nodes and complexification of the wave function.**

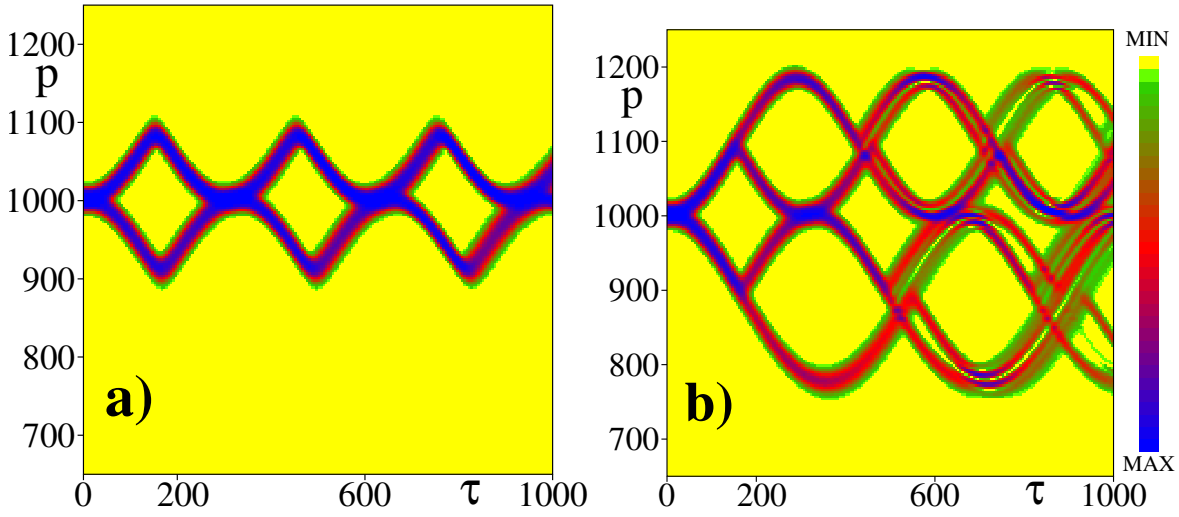

Figure 7: **Momentum probability distribution $\mathcal{P}(p,\tau)$ of a Gaussian wave packet vs time with $p_0 = 1000, \sigma_p^2 = 50$, and $\omega_r = 10^{-5}$ at (a) $\Delta = 0.3$, adiabatic motion, and (b) $\Delta = 0.1$, motion with nonadiabatic transitions. The color codes the values of $\mathcal{P}(p,\tau)$.**

The key result is that the squared angular amplitude of the u map is exactly the Landau–Zener parameter (16), i.e., $\Theta^2 = \kappa$

$$\arcsin u_m = \sqrt{\kappa} \sin \varphi_m + \arcsin u_{m-1}. \tag{17}$$

If $\kappa \simeq 1$, then the internal atomic variable $\arcsin u_m$ just after crossing the m-th node may take with the same probability practically any value from the range $[-\pi/2, \pi/2]$. It means semiclassically that the momentum of a ballistic atom changes chaotically upon crossing the field nodes. In accordance with the quantum formula (16), the corresponding atomic wave packet makes nonadiabatic transitions when crossing the nodes and splits at each node. As the result, the wave packet of a single atom becomes so complex that it may be called a chaotic one in the sense that it is much more complicated than the wave packets propagating adiabatically. Thus, nonadiabatic wave chaos and semiclassical dynamical chaos occur in the same range of the control parameters and are specified by the same Landau–Zener parameter $\kappa \simeq 1$. In two limit cases with $\kappa \ll 1$ and $\kappa \gg 1$ both the semiclassical and quantized translational ballistic motion are regular.